ELASTIC MATERIAL CONSTANTS OF LANGASITE-TYPE CRYSTALS DETERMINED BY ACOUSTIC WAVES

E. Chilla[1,2,*], **C. M. Flannery**[2,3], **H.-J. Fröhlich**[2], **J. Bohm**[4], **R.B. Heimann**[5], **M. Hengst**[5], **U. Straube**[6]
[1]Vectron International Tele Filter, Teltow, Germany
[2]Paul Drude Institute for Solid State Electronics, Berlin, Germany
[3]National Institute of Standards and Technology (NIST), Boulder, U.S.A.
[4]Institute for Crystal Growth, Berlin, Germany
[5]Department of Mineralogy, Freiberg University of Mining and Technology, Freiberg, Germany
[6]Department of Physics, Martin-Luther-University, Halle, Germany
[*]Email: chilla@telefilter.com

Abstract

We have determined the elastic constants of the langasite-type crystals $La_3Ga_5SiO_{14}$ (langasite-LGS), $La_3Ga_{5.5}Nb_{0.5}O_{14}$ (langanite-LGN), and $La_3Ga_{5.5}Ta_{0.5}O_{14}$ (langataite-LGT) from bulk acoustic wave measurements and angular dispersion measurements of surface guided acoustic modes. Starting with the elastic tensor determined from bulk acoustic waves we optimized the data set by investigating the influence of the elastic tensor components on the angular dispersion of surface guided waves. This procedure is particularly useful for accurate determination of the non-diagonal elements of the elastic tensor. Surface acoustic waves (SAW) and leaky waves were measured by thermoelastic laser excitation. The average measurement error is of about ± 1 m/s and the measurements are repeatable to this tolerance. The angular dependence of the velocity was obtained by mounting the sample on a computer controlled rotation stage. Phase velocity calculations based on the new set of constants show an increased agreement with experimental data compared to the data set derived from bulk waves and previously published material data.

Introduction

Single crystals with $Ca_3Ga_2Ge_4O_{14}$ (CGG)-type structure, have recently been intensively discussed as promising new materials for surface acoustic wave (SAW) devices. These crystals belong to the same trigonal crystal class as quartz. Hence similar acoustic properties are expected [1], [2], [3]. In particular, temperature compensated crystal cuts were predicted where the acoustic phase velocity slowly varies with temperature. Three additional advantages have been discussed so far: (i) The piezoelectric moduli are larger than for quartz. Hence, a moderately high electromechanical coupling coefficient is expected (ii) The SAW phase velocity is lower than for quartz. Since the finger width of interdigital transducers (IDTs) for SAW generation depends on the acoustic wavelength, SAW devices on CGG-type substrates have smaller sizes. (iii) In contrast to quartz, where a structural phase transition appears many CGG-type crystals show structural stability up to the melting point. Hence application at elevated temperatures, especially in sensing devices are possible.

The family of the CGG-type crystals covers more than 60 members. Here we report on the determination the elastic constants of LGS (langasite, $La_3Ga_5SiO_{14}$), LGN (langanite, $La_3Ga_{5.5}Nb_{0.5}O_{14}$), and LGT (langataite, $La_3Ga_{5.5}Ta_{0.5}O_{14}$) from the measurement of the phase velocity of surface guided acoustic waves.

Thermoelastic SAW Measurements

Surface guided acoustic modes were generated by 0.5 ns laser pulses (0.5 mJ pulse energy) from a Nitrogen laser (wavelength 337 nm) which is focused into a line shape on the sample surface. The sketch of the experimental setup is shown in Figure 1. The energy

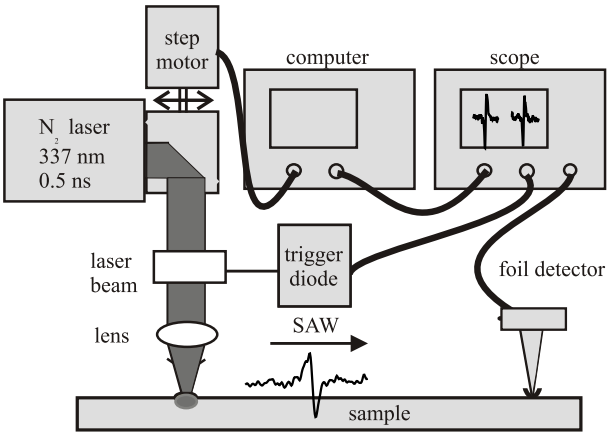

Figure 1: Thermoelastic setup of SAW measurement.

is absorbed as heat into a small volume at the sample surface. This causes a rapid expansion and contraction of the source which gives rise to acoustic wave packets propagating through the sample. Most of the energy goes into surface guided acoustic waves. These broadband SAW wave packets (typically 20-100 MHz frequency range) propagate across the sample surface

and are detected by a PVDF foil with steel-wedge transducer. The out-of-plane mechanical vibrations are converted to a voltage, amplified and stored by a digitizing oscilloscope [4], [5]. The sample is scanned relative to the laser beam and the SAWs are detected after different propagation distances (typically at 1 mm intervals over up to 10 mm propagation distance). The time delay between two wave packets is obtained from the peak of a cross-correlation of the signals. Knowing the difference in the propagation distance then yields the velocity. Each wave packet is cross-correlated with all the other wave packets and an overall velocity is obtained from a weighted mean of all the velocities obtained. The average measurement error is of about ± 1 m/s. The angular dependence of the velocity was obtained by mounting the sample on a computer controlled rotation stage. Figure 2 shows the angular phase velocity dispersion of LGS (square), LGN (up triangle), and LGT (down triangle) for the Z-cut. Due to the hexagonal symmetry a periodicity of 60 degrees is observed. The measured wave is a leaky SAW and the energy leakage into the substrate induces damping of the wave. However, for 0 degree and 30 degree propagation the damping is small and also the beam steering, i.e. deviation of group and phase velocity, can be neglected. When the propagation direction changes, the damping increases and the directions of the group velocity and phase velocity increasingly diverge. Consequently the signal to noise ratio reduces. Especially for the velocity minima, the beam steering rapidly increases when the propagation direction slightly changes. Hence, the signal at the detector reduces drastically entailing a reduced accuracy of the velocity measurement. This is the reason why for the angular range from 28 to 32 degrees only few velocity data where found and the deviation with respect to the calculated values is higher than for other angular ranges. For the X-cut shown in Figure 3 we have measured SAWs over a wide angular range for LGS and LGN. The velocity change is about 500 m/s for LGS and about 450 m/s for LGN and, hence, much higher than for the Z-cut. Furthermore, the measured velocity values for LGS, LGN and LGT are considerably smaller than for quartz, where the velocity range is 3852-3165 m/s and 4171-3685 m/s for the X- and Z-cut, respectively. For LGT, however, the lowest velocity was observed.

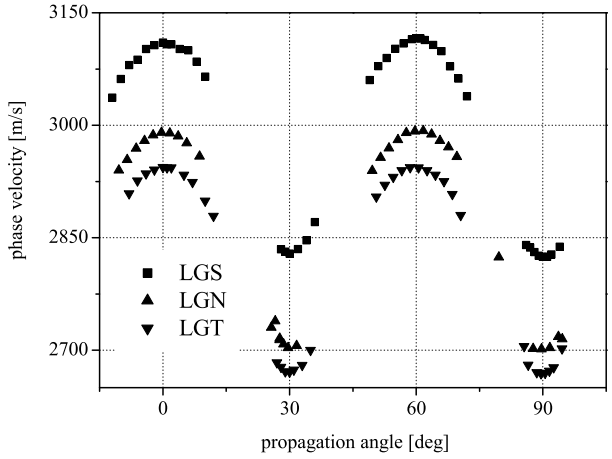

Figure 2: Angular dispersion of leaky SAWs on Z-crystal cut of LGS (square), LGN (up triangle), and LGT (down triangle).

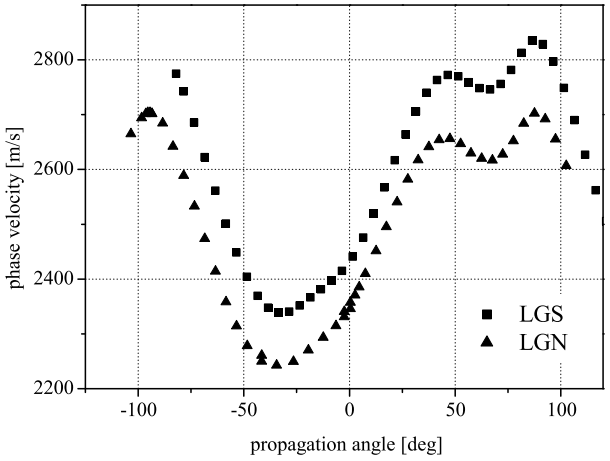

Figure 3: Angular dispersion of SAWs on X-crystal cut for LGS (diamonds) and LGN (squares).

The measurements were carried out on polished Z- and X-cut disks with a diameter of 15-20 mm and a thickness of 0.5-1 mm. Since LGS, LGN, and LGT are almost transparent at a laser wavelength of 337 nm, the samples were coated with a 50 nm Al layer to increase the UV absorption efficiency. The metal film, however, short-circuits the piezoelectric field. Hence the phase velocities will be reduced by $\Delta v = vk^2/2$ as compared to the velocity v at the free crystal surface, with k^2 being the electromechanical coupling factor. For langasite-type crystals, the coupling factor, mainly determined by the piezoelectric constants, is some tenth of a percent. Hence, the metal film can change the sound velocities by some m/s. Consequently, for accurate velocity calculations the effect of short-circuiting must be considered by choosing the correct electrical boundary conditions during the analysis of the data. The velocity also changes due to the mass loading by the thin Al layer. In the frequency range lower than 100 MHz this effect is less than 1 m/s and was, therefore, neglected.

Elastic constants recovery

The elastic properties of single crystalline materials are determined by the elastic stiffness tensor c_{ij}. For symmetry reasons, six independent elastic components

exist for the crystal class *32* , i.e. c_{11}, c_{12}, c_{13}, c_{14}, c_{33}, and c_{44}. The total stiffness tensor consists of 18 non-vanishing components and can be written in a symmetrical 6×6 matrix form with $c_{66} = (c_{11} - c_{12})/2$. The most common method for the extraction of the elastic constants is based on the phase velocity measurement of ultrasonic waves. In principle, the elastic constants can be determined by interactively solving the direct problem, i.e. calculating the phase velocity for a given set of elastic parameters, and finding the minimum of the deviation with respect to the measured velocity data. Since this is a multi-parameter non-linear procedure, the uncertainties of the input parameters, in particular the errors of the phase velocity measurement, can have a significant impact on the results. Hence, it is essential to operate with high accuracy velocity data.

In contrast to bulk acoustic waves, in almost all but the most simple cases the elastic constants cannot be recovered from SAW data analytically. Hence, the inverse problem is solved by interactively calculating the SAW velocity and optimizing the elastic parameters. We started the optimization with the set of constants determined from the bulk wave data [2], [3]. For optimization of the elastic constants by means of the SAW data we first analyzed the velocity change, when one particular constant is changed, independently. Figure 4 shows the sensitivity of the leaky SAW on the Z-cut LGS when the elastic parameters are decreased by 2%. A smaller constant can decrease as well as increase the velocity. In general, c_{11}, c_{44}, and c_{12} have the most significant influence on the velocity. However, for the leaky SAW (Fig. 4) c_{11} dominates within the angular range at about 0 (60) degree and c_{44} at about 30 degree. The decrease of c_{12} reduces the velocity. For

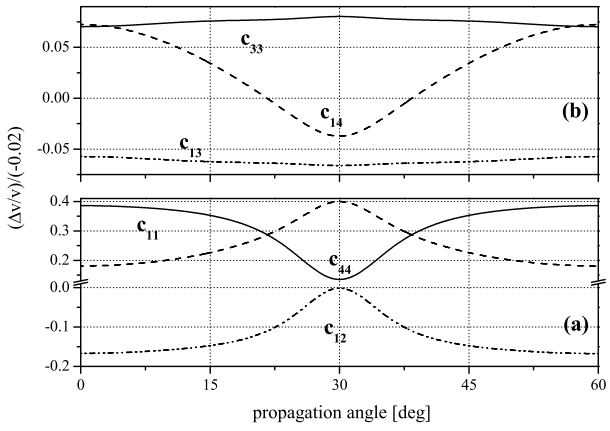

Figure 4: Propagation direction dependence of velocity change for Z-cut LGS when (a) c_{11} (solid), c_{12} (dashed), c_{44} (dash-dot-dot) and (b) c_{33} (solid), c_{14} (dashed), c_{13} (dash-dot-dot) are reduced by 2%.

the wave propagation along 30 degree the velocity is almost independent on c_{12} variation. The influence of

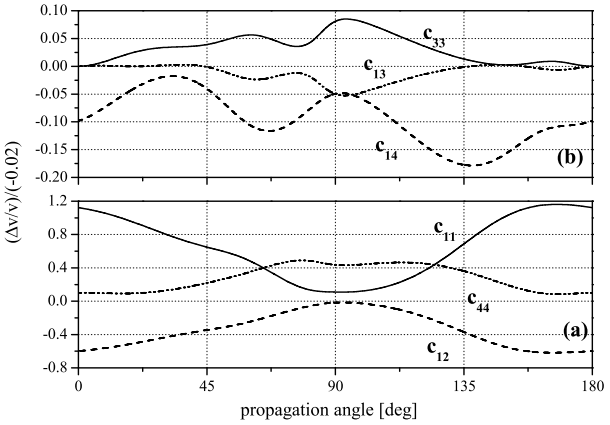

Figure 5: Propagation direction dependence of velocity change for X-cut LGS when (a) c_{11} (solid), c_{12} (dash), c_{44} (dash-dot-dot) and (b) c_{33} (solid), c_{14} (dash), c_{13} (dash-dot-dot) are reduced by 2%.

the change of c_{33} on the leaky SAW velocity is almost constant and opposite with respect to the influence of c_{13} over the whole angular range. The change of c_{14} can increase as well as decrease the velocity depending on the propagation direction, however, for the Z-cut it alters the velocity very little only. These results

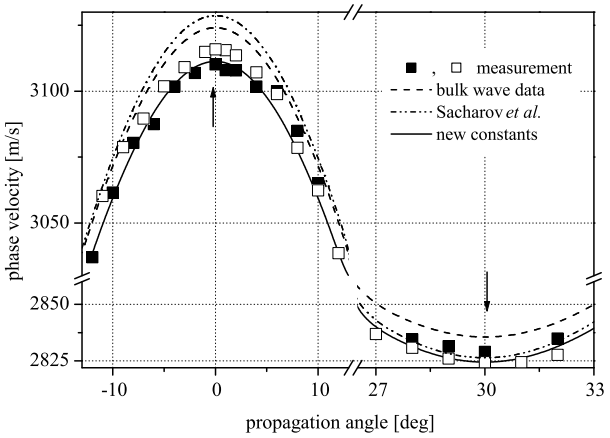

Figure 6: Leaky SAW on Z-cut LGS (c.f. Fig. 2). Dashed and solid lines represent calculations for elastic constants derived from bulk waves and optimized values regarding SAWs, respectively. Arrows mark data applied for inverse recovering of elastic constants. Dotted line represents calculations based on material data reported by Sacharov *et al.*

indicate that for the accurate recovery of the elastic parameters, various crystal cuts are needful. We have additionally investigated the SAW sensitivity for the X-cut (Fig. 5). Here, the elastic parameters show a quite different dependence compared to the Z-cut. The influence of c_{44} on the velocity is much more significant than on the Z-cut and dominates in the wide angular range from -45 to +45 degree. Also the influence of

c_{14} is higher for certain propagation angles. Since the influence of the stiffness variation is quite different for different crystal cuts and propagation angles, the optimization procedure will change the constants predominantly for a particular angle. For the mean square fit estimation of the calculated and measured phase velocity data we have solved the system of equations $p_{mn}\Delta_n - y_m = 0;\ \ m = 1..9,\ n = 1..6$, considering velocity data of four SAWs, two leaky SAWs, one degenerated shear wave and two longitudinal BAWs propagating along the X- and Z-axes, respectively. The

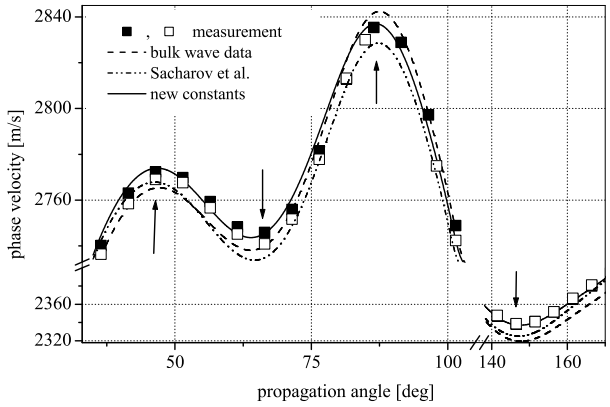

Figure 7: SAW angular dispersion on X-cut LGS. Dashed line: calculation for bulk wave data; dotted line: calculations based on material data reported by Sacharov *et al.*; solid line: optimized constants regarding SAW data.

coefficients p_{nm} represent the numerical values of the velocity sensitivity $(\Delta v/v)/(\Delta c_{ij}/c_{ij})$ at selected surface wave propagation directions and p_{71}, p_{85}, and p_{96} are the equivalent bulk wave sensitivities. These directions coincide with maxima and minima in the angular dependence of velocity (arrows in Figure 6 and Figure 7). The relative changes of elastic stiffness are: $\Delta_1 = \Delta c_{11}/c_{11}$, $\Delta_2 = \Delta c_{12}/c_{12}$, $\Delta_3 = \Delta c_{13}/c_{13}$, $\Delta_4 = \Delta c_{14}/c_{14}$, $\Delta_5 = \Delta c_{33}/c_{33}$, $\Delta_6 = \Delta c_{44}/c_{44}$, $\Delta_7 = \Delta_1$, $\Delta_8 = \Delta_5$, $\Delta_9 = \Delta_6$, and y_m is the correction value of the velocity. Then the minimum of the error function is calculated by iterative variation of the Δ_n. In case of LGT the coefficient p_{mn}[LGN] was applied. This is reasonable, since the sensitivity dependence of the velocities are very similar for LGS, LGN, and LGT. The new elastic constants are shown in Table 1. For illustration, the dashed line in Figure 6 and Figure 7 displays the angular dispersion of the phase velocity calculated for the initial set of elastic constants determined from bulk measurement. In general, the data fit the experimental behavior well. However, for the Z-cut (Fig. 6) the values are slightly higher while for the X-cut (Fig. 7) they are slightly higher for about 90 degree and slightly lower otherwise. The deviation

Table 1: Material constants of $La_3Ga_5SiO_{14}$, $La_3Ga_{5.5}Nb_{0.5}O_{14}$, and $La_3Ga_{5.5}Ta_{0.5}O_{14}$.

	LGS	LGN	LGT
$\rho\ [kg/m^3]$	5733	5905	6145
$\varepsilon_1/\varepsilon_0$	19.2	20.7	19.6
$\varepsilon_3/\varepsilon_0$	50.7	79.0	76.5
$e_{11}\ [C/m^2]$	0.43	0.513	0.508
$e_{14}\ [C/m^2]$	-0.148	-0.108	-0.028
$c_{11}\ [GPa]$	189.8	189.3	188.9
$c_{12}\ [GPa]$	105.8	108.9	108.6
$c_{13}\ [GPa]$	102.2	99.31	104.4
$c_{14}\ [GPa]$	14.4	13.4	13.74
$c_{33}\ [GPa]$	263.5	259.74	264.5
$c_{44}\ [GPa]$	54.16	49.76	51.29
$c_{66}\ [GPa]$	42.02	40.17	40.19

between the calculated and the measured data is indeed larger than the experimental accuracy of the SAW measurement. Also, the deviation is dependent on the propagation angles. The accuracy is also higher then the calculations based on the sets of material constants reported by Sacharov *et al.* [6].

References

[1] J. Bohm, R. B. Heimann, M. Hengst, R. Roewer, and J. Schindler, J. Crystal Growth **204**, 128 (1999).

[2] J. Bohm, E. Chilla, C. Flannery, H.-J. Fröhlich, T. Hauke, R. B. Heimann, M. Hengst, and U. Straube, J. Cryst. Growth, **216**, 293 (2000).

[3] E. Chilla, C. Flannery, H.-J. Fröhlich, and U. Straube, J. Appl. Phys. **90**, 6084 (2001).

[4] D. Schneider, T. Schwarz, H.-J Scheibe, and M. Panzer, Thin Solid Films **295**, 107 (1997)

[5] C. M. Flannery, E. Chilla, S. Semenov, and H.-J. Fröhlich, Proc. IEEE Ultrason. Symp., 409 (1999).

[6] S. Sacharov, P. Senushencov, A. Medvedev, and Yu. Pisarevski, Proc. IEEE Int. Freq. Contr. Symp., 647 (1995)